

# Supporting Information - A Bayesian approach to extracting kinetic information from enzymatic reaction networks

Mathieu G. Baltussen<sup>1</sup>      Jeroen van de Wiel<sup>1</sup>      Cristina Lía Fernández Regueiro<sup>1</sup>  
Miglė Jakštaitė<sup>1</sup>      Wilhelm T.S. Huck<sup>1,\*</sup>

<sup>1</sup> Institute for Molecules and Materials, Radboud University Nijmegen, Nijmegen, the Netherlands;

\* Correspondence: Wilhelm T.S. Huck <w.huck@science.ru.nl>

## Contents

<b>Materials and Instrumentation</b>	<b>S3</b>
Materials . . . . .	S3
Enzymes . . . . .	S3
Substrates . . . . .	S3
Instrumentation & Quantification protocols . . . . .	S3
Flow setup . . . . .	S3
Spectroscopy . . . . .	S3
High-performance liquid chromatography . . . . .	S5
G6P-DH assay . . . . .	S5
<b>Production and characterisation of polyacrylamide-enzyme beads</b>	<b>S6</b>
Microfluidic devices fabrication for beads production . . . . .	S6
Method 1: Enzyme-first functionalization . . . . .	S6
Synthesis 6-acrylaminohexanoic acid succinate (AAH-Suc) linker . . . . .	S6
Enzyme functionalization . . . . .	S6
General Enzyme Immobilization During Polymerization (EIDP) method . . . . .	S6
Method 2: . . . . .	S7
Empty bead production method . . . . .	S7
General Enzyme Immobilisation after Polymerisation (EIAP) Method . . . . .	S7
Overview of PEBs . . . . .	S7
<b>Overview of experiments</b>	<b>S8</b>
<b>Overview of computational methods</b>	<b>S9</b>
<b>Extended iterative combination of experiments</b>	<b>S9</b>
<b>Model details &amp; sampling diagnostics</b>	<b>S11</b>
Obtaining improved accuracy from correlated parameter estimates . . . . .	S11
Model . . . . .	S11
Diagnostics . . . . .	S11
Combining diverse experimental datasets . . . . .	S13
Model . . . . .	S13
Diagnostics . . . . .	S13
Comparing reaction mechanism hypotheses . . . . .	S15

Models . . . . .	S15
Hypothesis 0 . . . . .	S15
Hypothesis 1 . . . . .	S15
Hypothesis 2 . . . . .	S18
Hypothesis 3 . . . . .	S18
Hypothesis 4 . . . . .	S18
<b>References</b>	<b>S25</b>

# Materials and Instrumentation

## Materials

All chemicals and reagents were used as received from commercial suppliers without any further treatment unless stated otherwise.

## Enzymes

The enzymes immobilized on PEBs were purchased from Merck Sigma-Aldrich. Specifically:

- Lyophilized Trypsin (Tr) from bovine pancreas (product no. T1426)
- Lyophilized Glucose Dehydrogenase (GDH) from *Pseudomonas* sp. (product no. 19359)
- Lyophilized Hexokinase, type F-300 (HK) from *Saccharomyces cerevisiae* (product no. H4502)
- Lyophilized Glucose-6-phosphate dehydrogenase (G6P-DH) from *Leuconostoc menesteroides* (product no. G8529)

Trypsin reactions was conducted in a 200 mM Tris buffer, pH 7.8, with 20 mM of CaCl<sub>2</sub>. GDH, HK and G6P-DH reactions were conducted in a 200 mM Tris buffer, pH 7.8, with 10 mM of MgCl<sub>2</sub>.

## Substrates

The substrates Cbz-Arg-AMC (R-AMC, CAS: 3701-04-6, New catnr: 4002540.0050) and Suc-Ala-Ala-Ala-AMC (AAA-AMC, CAS 73617-90-0, New catnr: 4006305.0050) were purchased from BioConnect B.V. and were dissolved as 150 mM stock in anhydrous DMSO and kept frozen at -20°C.

The substrates employed for all metabolic enzymatic reactions were:

- Glucose (anhydrous) (Merck product no. 1083370250)
- glucose-6-phosphate hydrate (Sigma Aldrich product no. G7250)
- ATP disodium salt (Sigma Aldrich product no. A26209)
- ADP monosodium salt (Sigma Aldrich product no. A2754)
- NAD<sup>+</sup> (Roche product no. 10127965001)
- NADH disodium salt (Roche product no. 10107735001)
- NADP<sup>+</sup>disodium salt (Roche product no. 10128031001)
- NADPH tetrasodium salt (Roche product no. 1010724001)

## Instrumentation & Quantification protocols

### Flow setup

A custom made CSTR (see Figure S1 for the design schematic, effective volume 100 $\mu$ L) was charged with PEBs (in a ratio of 1:31 mg beads:injection volume). The openings of the reactor were sealed with Whatman Nuclepore Track-Etch polycarbonate membranes (5  $\mu$ m poresize, cat. number 10417414) to prevent outflow of PEBs. To subject the CSTR to various flow conditions we used Cetoni Low-Pressure High-Precision Syringe Pumps neMESYS 290N and gastight Hamilton syringes, with all flowrates programmed using the Cetoni neMESYS software. For all methods of offline detection, the outflow of the CSTR was connected to a BioRad 2210 Fraction collector, collecting for 7.5 (absorbance) or 10 minutes (HPLC) per fraction. This experimental setup is shown in Figure S2a-b

### Spectroscopy

**Offline fluorescence** Collected fractions were pipetted onto a microplate (Greiner Bio One, black, polystyrene, 96 flat bottom chimney wells) at 60  $\mu$ L per well. Fluorescence measurements for enzyme activity determination were performed with a Tecan Spark 10M plate reader. The fluorescence intensity of wells containing 30-200  $\mu$ L of the reaction mixture was monitored for 1-4 min (shaking 3s/orbital mode/amplitude 4mm) at 23 °C using top or bottom reading mode, at  $\lambda_{ex}/\lambda_{em} = 380\text{nm}/460\text{nm}$  for 7-amino-4-methylcoumarin (AMC) based substrates.

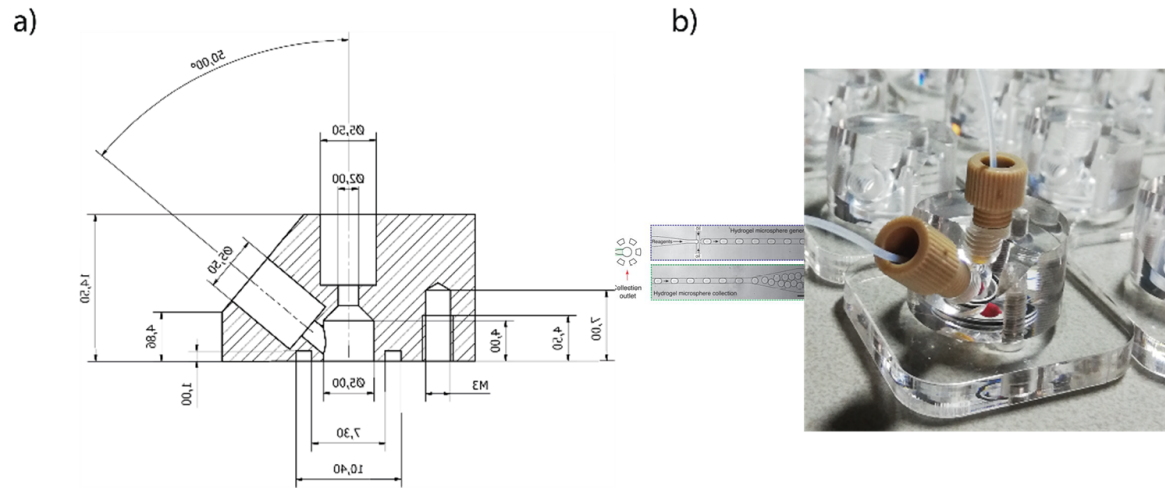


Figure S1: (a) Schematic overview of the CSTR. (b) Photograph of the CSTR

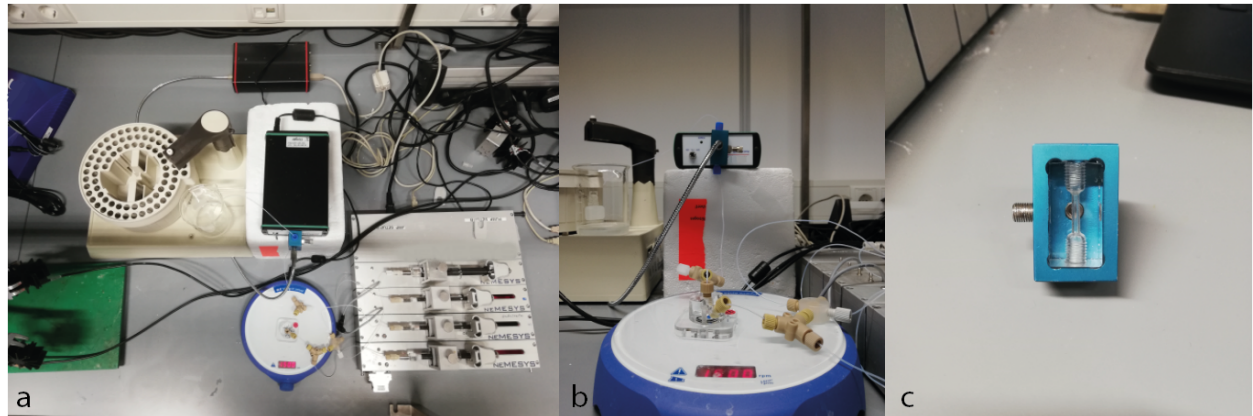


Figure S2: (a) Overview of the experimental setup, with left the fraction collection, lower center the CSTR on a stirring plate, and lower right the neMESYS pump system. (b) Close-up of the CSTR connected to input and output tubing. (c) Close-up of the flow cuvette used for online absorbance detection, provided by LabM8

**Offline absorbance** Collected fractions were pipetted onto a microplate (Greiner Bio One, transparent, polystyrene, 96 flat bottom chimney wells) at 60  $\mu L$  per well. The absorbance of each sample at 340 nm was measured in a TECAN SPARK M10 platereader. Using a calibration curve, the absorbance data was converted to NADH concentration.

**Online absorbance** Absorbance in flow experiments was continuously measured at the reactor's output with a custom made flow cell kindly provided to us by LabM8 (shown in Figure S2c), connected to an AvaLight 355 nm LED lamp. Absorbance at 380 nm was detected using an AvaSpec-2048 with 1,005 ms integration time and averaging at 200 times per recorded datapoint. Using a calibration curve, the absorbance data was converted to NADH concentration.

### High-performance liquid chromatography

High-performance Liquid Chromatography (HPLC) was performed using Shimadzu NexeraX3/Prominence system under a 0.9 mL/min flow at 45 °C with a Shimadzu WAX-1 column. For the Shimadzu system, an injection volume was subjected to a 25 min gradient program was used starting from 20 mM of potassium phosphate at pH 7.0

- 1 min – 20 mM at pH 7.0
- 16 min – 480 mM at pH 6.8
- 19 min – 480 mM at pH 6.8
- 22 min – 20 mM at pH 7.0
- 25 min – 20mM at pH 7.0

Retention time of ADP is at 8.8 minutes, ATP at 15.5 minutes.

### G6P-DH assay

Collected fractions were pipetted onto a microplate (Greiner Bio One, transparent, polystyrene, 96 flat bottom chimney wells) at 60  $\mu L$  per well. To these wells was added an 20  $\mu L$  of 5 mM of NADP+ and 1  $\mu L$  of 500 u/mL of G6P-DH. The absorbance of each sample at 340 nm was continuously measured in a TECAN SPARK M10 platereader. Using a calibration curve, the absorbance data was converted to NADPH concentration. We assumed this NADPH concentration equivalent to G6P concentration.

# Production and characterisation of polyacrylamide-enzyme beads

## Microfluidic devices fabrication for beads production

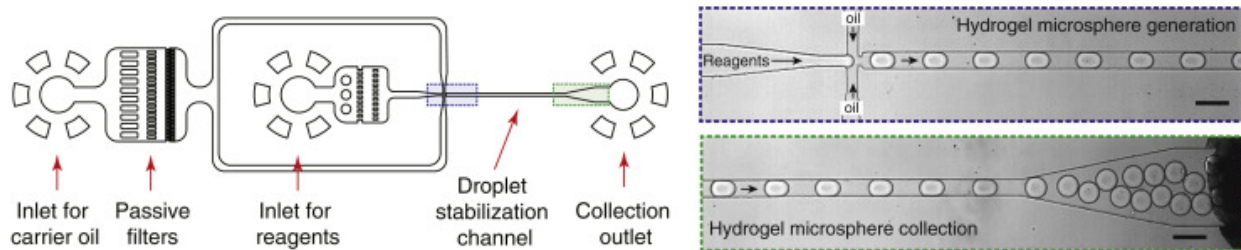


Figure S3: Schematic of the microfluidic device for droplets production (*adaptated from<sup>1</sup>*)

Microfluidic devices, designed according to the scheme shown in Figure S3<sup>1</sup>, were produced in silicon wafers by photo and soft lithography, with different orifice sizes (20-80 $\mu\text{m}$ ) at the T-junction, for droplet formation. After that, the wafers were used for the production of polydimethylsiloxane (PDMS) devices. The PDMS replicas were separated from the wafer, and inlets and outlets of 1mm inner diameter were punched. After the replica was bonded by oxygen plasma treatment to a glass slide, channels were coated with 2% 1H,1H,2H,2H-Perfluoro-octyltriethoxysilane to make them hydrophobic<sup>2</sup>.

### Method 1: Enzyme-first functionalization

This method was used for the synthesis of PEBs containing Trypsin.

#### Synthesis 6-acrylaminohexanoic acid succinate (AAH-Suc) linker

N-6-acryloyl amido hexanoic acid (30 mg, 0.172 mmol, 1 eq) and N-Hydroxy succinimide (20mg, 0.172 mmol, 1eq) were added in a large glass vial and brought under N<sub>2</sub> atmosphere. Subsequently, they were dissolved in 1 mL of anhydrous DMF and cooled down to 0°C. Then, N, N'-dicyclohexylcarbodiimide (DCC, 38mg, 0.172mmol, 1eq) was added, and the vial was sealed and left to stir at 0°C for one hour. Subsequently, the reaction was brought to 4°C and stirred for 16h. The reaction mixture was assumed quantitative and immediately used for enzyme functionalisation without further analysis<sup>3</sup>.

#### Enzyme functionalization

The desired enzyme (1 eq) was added to a falcon tube containing 0.1 M NaHCO<sub>3</sub> (4mL), followed by addition of AAH-Suc (7.5 eq) in DMF. The mixture was left to stir at 21 °C for 1 h, after which the reaction mixture was dialysed and lyophilised.

#### General Enzyme Immobilization During Polymerization (EIDP) method

An emulsion of monodisperse water-in-oil droplets was produced by using the microfluidic device described above with a 20  $\mu\text{m}$ -wide T-junction, following an adapted procedure from Rivello et al.<sup>[3]</sup> The reagents phase used for hydrogel formation was composed by 9.7% (w/v) acrylamide, 0.4% (w/v) bisacrylamide, 1.5% (w/v) 2,2'Azobis(2-methylpropionamidine) dihydrochloride (AAPH) and 0-8% (v/v) of a solution of functionalized enzyme (100  $\mu\text{M}$ ). The oil phase was composed of fluorinated fluid HFE-7500 (3M) and 1.5% (v/v) Pico-Surf™ 1. The flow rates used to produce monodisperse beads of 50 $\mu\text{m}$  average diameter were 600 $\mu\text{L}/\text{h}$  (Q<sub>w</sub>) for the reagents phase and 900 $\mu\text{L}/\text{h}$  for the oil phase (Q<sub>o</sub>). The emulsion of droplets created in the microfluidic device was collected in an Eppendorf with 100 uL mineral oil to avoid evaporation and breaking the emulsion and polymerised for 10 minutes under UV light. After polymerisation, beads were washed three times with 20% (v/v) 1H,1H,2H,2H perfluorooctanoic (PFO) in HFE-7500 oil to break the emulsion. The obtained beads were then washed three times with 1% (v/v) Span 80 in heptane, three times with 0.1% (v/v) Triton X-100 in miliQ and three times with Milli-Q. After every washing step, the beads were

centrifugated 30 seconds at 5000 rcf, and the supernatant was removed by pipetting. The resulting beads were freeze-dried and re-dissolved in miliQ at a concentration of  $0.0322\text{mg}/\mu\text{L}$ . Bead size was obtained after freeze-drying by imaging with a light microscope with a 40x objective lens. The average bead size was  $50\ \mu\text{m}$ .

## Method 2:

This method was used for the synthesis of PEBs containing GDH, HK, and G6PDH.

### Empty bead production method

The microfluidics device described above was used to produce gel beads with a  $20\ \mu\text{m}$  wide T-junction, following an adapted procedure from<sup>2</sup>. The gel solution phase consisted of 9.6% (w/v) acrylamide, 0.4% (w/v) N,N'-methylenbisacrylamide, 0.5% (w/v) acrylic acid and 1.5% (w/v) 2,2'-Azobis(2-methylpropionamidine) dihydrochloride. The oil phase contained 1.5% (v/v) Pico-Surf™ 1 in fluorinated fluid HFE-7500 (3M). The flow rates for gel phase and oil phase were  $600\ \mu\text{L}/\text{h}$  and  $900\ \mu\text{L}/\text{h}$ , respectively. The outflow emulsion was collected in the tube which was filled with  $100\ \mu\text{L}$  mineral oil. Afterwards beads were polymerised using UV lamp for 10 minutes at 70% gain. After polymerisation the lowest layer containing fluorocarbon phase was carefully removed with a P200 pipette. The remaining beads were washed 3 times with 20% (v/v) 1H,1H,2H,2H-Perfluoro-1-octanol in HFE-7500 (3M), then 3 times with 1% (v/v) Span 80 in hexane, 3 times with 0.1% (v/v) Triton X-100 in Milli-Q and finally 3 times with Milli-Q. Every washing step was finalised with mixing the tube using vortex, centrifuging at  $5000\ \times g$  for 3 min and removing the layer which was not containing beads. Furthermore, beads were flash frozen using nitrogen and freeze dried overnight. After re-wetting beads, their size was determined using light microscope with 40x magnitude objective. The average size was  $50\ \mu\text{m}$  in diameter.

### General Enzyme Immobilisation after Polymerisation (EIAP) Method

Empty acrylamide beads were re-dissolved in Milli-Q at a concentration of  $0.0322\ \text{mg}/\mu\text{L}$ . 1-(3-Dimethylaminopropyl)-3-ethylcarbodiimide hydrochloride (100 mM) and N-Hydroxysuccinimide (100 mM) were added to the reaction mixture. The total volume of the activation solution was 5-fold of the beads volume. The reaction mixture tube was put on the roller bank for 30 min. After this, beads were centrifuged at  $5000\ \times g$  for 3 min. The supernatant was carefully removed using P200 pipette. Beads were washed 3 times by adding Milli-Q, mixing using vortex, centrifuging and removing the supernatant. Specific to each batch of PEBs, a certain amount of enzyme was added to the beads (see Table S1). The tube was put on the roller bank for 2 h coupling step. Sequentially, beads were washed 8 times by adding Milli-Q, centrifuging and removing the supernatant. Finally, beads were flash frozen using nitrogen and freeze dried overnight.

## Overview of PEBs

Table S1: Overview of PEB batches

Enzyme	Batch number	Enzyme concentration added	Volume per mg of beads
GDH	1	0.54 kUnit/mL	$100\ \mu\text{L}/\text{mg}$
	2	2 kUnit/mL	$100\ \mu\text{L}/\text{mg}$
	3	1 kUnit/mL	$100\ \mu\text{L}/\text{mg}$
HK	1	1 kUnit/mL	$100\ \mu\text{L}/\text{mg}$
G6P-DH	1	1 kUnit/mL	$100\ \mu\text{L}/\text{mg}$

## Overview of experiments

Processed datafiles from these experiments can be found on the accompanying github repository in the `data` folder as csv-files. The files are directly used during analysis performed in the Jupyter notebooks.

In the tables below, the volume refers to the volume of PEBs suspension injected into the CSTR, where the PEBs suspension itself is created by suspending 1 mg of dry PEBs in 31  $\mu L$  buffer, or other quantities in the same ratio (1:31). The batch refers to the batch of PEBs, which can contain different effective enzyme concentration. See Table S1 for an overview of all PEB batches.

Table S2: Overview of single-enzyme experiments

Code	flowrate ( $\mu L/h$ )	enzyme	volume ( $\mu L$ )	batch	inputs	observables	observation techniques
SNCA14	750	GDH	10	1	G, NAD	NADH	offline abs.
SNCA15	750	GDH	10	1	G, NAD	NADH	offline abs.
SNCA17	750	HK	10	1	G, ATP	G6P	G6P assay
SNCA18	750	HK	1	1	G, ATP	G6P	G6P assay
SNKS03	750	HK	1	1	G, ATP	G6P	G6P assay
SNKS04	750	HK	1	1	G, ATP	G6P,ATP	G6P assay, HPLC
SNKS08	750	G6PDH	10	1	G6P, NAD	NADH	offline abs.
SNKS11	750	GDH	0.5	2	G, NAD	NADH	online abs.
SNKS12	750	GDH	0.5	2	G, NAD	NADH	online abs.
SNKS18	750	GDH	2.0	3	G, NAD	NADH	offline abs.
SNKS20	750	G6PDH	2.0	1	G6P, NAD	NADH	online abs.

Table S3: Overview of multi-enzyme experiments

Code	flowrate ( $\mu L/h$ )	enzymes	volumes ( $\mu L$ )	batches	inputs	observables	observation techniques
SNKS06	750	GDH, HK	10.0, 1.0	1, 1	G, NAD, ATP	NADH, ADP	online abs., HPLC
SNNS002	750	GDH, HK	0.5, 1.0	2, 1	G, NAD, ATP	NADH	online abs.
SNNS003	750	GDH, HK	0.25, 1.5	2, 1	G, NAD, ATP	NADH	online abs.
SNNS004	750	GDH, HK	0.333, 1.33	2, 1	G, NAD, ATP	NADH	online abs.
SNNS005	750	GDH, HK	0.666, 0.666	2, 1	G, NAD, ATP	NADH	online abs.
SNNS006	750	GDH, HK	0.75, 0.5	2, 1	G, NAD, ATP	NADH	online abs.
SNNS007	750	GDH, HK	0.5, 1.0	2, 1	G, NAD, ATP	NADH	online abs.

## Overview of computational methods

Python scripts and Jupyter notebooks were used to create the Bayesian models and perform inference and predictive sampling. All computational studies were performed with Jupyter notebooks. Datasets were loaded in from csv-files with Pandas, and if relevant, concatenated together into larger objects.

The Bayesian model, including the determination of prior probabilities and likelihood function, was created using PyMC3<sup>4</sup>. Generally, prior probabilities for Michaelis-Menten parameters were chosen as uniform distributions over a specified interval. These distributions were used as uninformative priors to ensure no subjective information would enter the model, while guaranteeing correct sampling and estimation of parameters. Priors for the uncertainty estimations (denoted by `sigma` in the notebooks) were given an exponential distribution, which also acted as an uninformative distribution, while guaranteeing correct sampling and convergence. In larger models, where multiple likelihoods were combined, hyperpriors were placed on the  $k_{cat}$  and  $\sigma$  priors to increase convergence of the sampling algorithm.

All sampling was performed using the No-U-Turn Sampler (NUTS)<sup>5</sup>, which is an adaptive step-size Hamiltonian Monte Carlo sampler. When (automatically, or via a custom operator) the gradients of the likelihoods with respect to the kinetic parameters were given, this sampling method is much more efficient than a classical Metropolis Monte Carlo sampler, showing faster convergence and requiring less samples for precise posterior estimations. Generally, sampling was performed using 4 or 8 independent chains on 4 or 8 cpu cores, all with 1000 tuning steps, and 1000 sampling steps, and a target step acceptance probability of 0.95. These values were found to yield good sampling results without becoming computationally inefficient.

For likelihood calculations of partially observable ERNs, a custom steady-state likelihood operator was written in Theano, according to description given in the manuscript. This operator is freely available from the public github repository at <https://github.com/mgbaltussen/BayERN>.

The samples obtained from the posterior distribution were further analysed using standard statistical tools in Python, the Numeric Python package and the Scientific Python package (NumPy and Scipy)<sup>6</sup>. To ensure the accessibility and reproducibility of these results the datasets and Jupyter notebooks, used for the analysis and creation of figures found in the publication, are made available as additional Supporting Information, and directly on github at [https://github.com/huckgroup/Bayesian-enzymatic-networks\\_manuscript\\_2022](https://github.com/huckgroup/Bayesian-enzymatic-networks_manuscript_2022). This repository also includes version information for all software dependencies.

PDF reproductions of example notebooks with explanation (`example_simple.ipynb` and `example_complex.ipynb`) are also included in the appendix of this supporting information.

## Extended iterative combination of experiments

See Figure S4 for an extended version of the figure, showing posterior updating per iteration of new experiment.

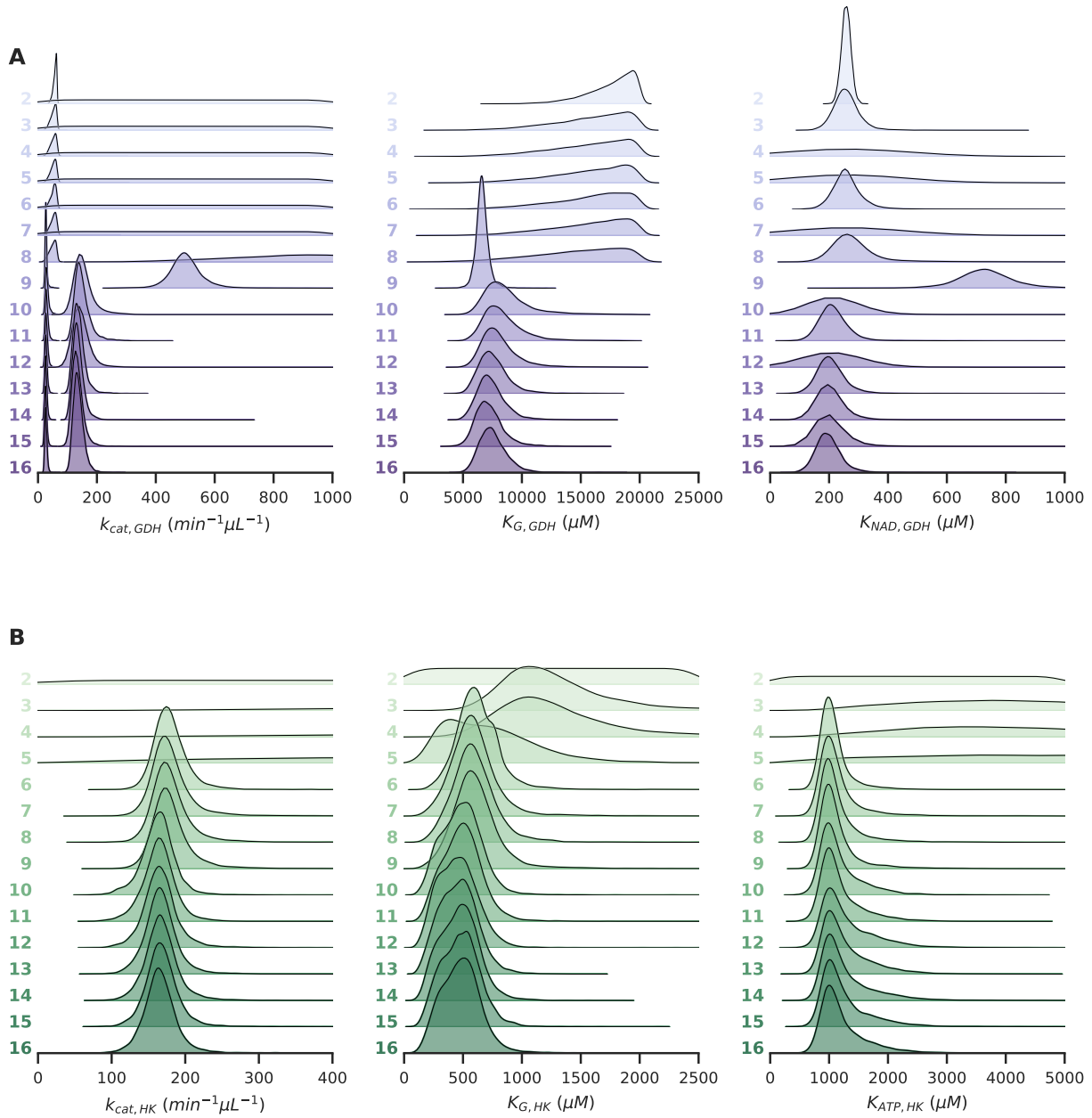


**Figure S4: Extended iterative posterior updating** (a,b) Posterior parameter estimates obtained from the model combining all three (GDH, HK, GDH+HK) observation likelihoods. For every parameter, the distributions are shown for 15 different datasets, with each following dataset containing an extra experiment, added in chronological order. Distributions are shifted and scaled to increase visibility. For the GDH  $k_{cat}$ , two estimates are obtained because PEBs with two different enzyme concentrations were used in different experiments.

## Model details & sampling diagnostics

### Obtaining improved accuracy from correlated parameter estimates

#### Model

The cleavage of R-AMC to AMC by the peptidase Trypsin was modelled following a Michaelis-Menten rate equation with an additional term describing uncompetitive inhibition by the inhibitor AAA-AMC. This results in the following system of ODE's:

$$\mathbf{f}(\mathbf{C}, \phi, \theta) : \begin{cases} \frac{d[P]}{dt} = \frac{E \cdot k_{cat} \cdot [S]}{K_M + [S] \cdot (1 + [I]/K_I)} - k_f [P] \\ \frac{d[S]}{dt} = \frac{-E \cdot k_{cat} \cdot [S]}{K_M + [S] \cdot (1 + [I]/K_I)} + k_f ([S]_{in} - [S]) \end{cases}$$

where  $[S]$  is the concentration of the substrate R-AMC,  $[P]$  the concentration of the product AMC, and  $[I]$  the concentration of the inhibitor AAA-AMC. This system contains 3 kinetic parameters that need to be inferred,  $\phi = \{k_{cat}, K_M, K_I\}$ , and 4 control parameters  $\theta = \{E, k_f, [S]_{in}, [I]\}$ . The measurements of the observed product concentration are assumed to have normal-distributed noise  $[P]_{obs} \sim N([P]_{ss}, \sigma)$  with a mean equal to the true steady-state concentration and an unknown standard-deviation  $\sigma$ . As priors for all 3 kinetic parameters, uninformative uniform distributions are used, with the following upper and lower boundaries:

$$\begin{aligned} P(k_{cat}) &= \mathcal{U}(0, 500) \\ P(K_M) &= \mathcal{U}(0, 500) \\ P(K_I) &= \mathcal{U}(1000, 10000) \end{aligned}$$

As prior for the noise estimate sigma, an uninformative exponential distribution is used:

$$P(\sigma) = \text{Exp}(10)$$

The full posterior is described by

$$\begin{aligned} P(k_{cat}, K_M, K_I, \sigma | [P]_{obs}, E, k_f, [S]_{in}, [I]) &\propto \prod_i P(\phi_i) \mathcal{L}(y, \phi) \\ &\propto P(k_{cat}) P(K_M) P(K_I) P(\sigma) \mathcal{N}([P]_{ss} - [P]_{obs}, \sigma) \end{aligned}$$

where  $[P]_{ss} = g(\phi, \theta)$  is the steady-state solution of  $\mathbf{f}(\mathbf{C}, \phi, \theta)$ .

#### Diagnostics

	Chains	Tuning steps	Draws	Mean acceptance rate	Divergences
0	4	1000	1000	0.949	0

Table: Sampling statistics for manuscript Figure 1

	mcse_mean	mcse_sd	ess_bulk	ess_tail	r_hat
k_cat	0.09	0.07	1129.0	1391.0	1.0
K_M	0.27	0.19	1276.0	1408.0	1.0
K_I	16.52	12.14	1615.0	1312.0	1.0
sigma	0.0	0.0	1473.0	1837.0	1.01

Table: Sampling diagnostics for manuscript Figure 1

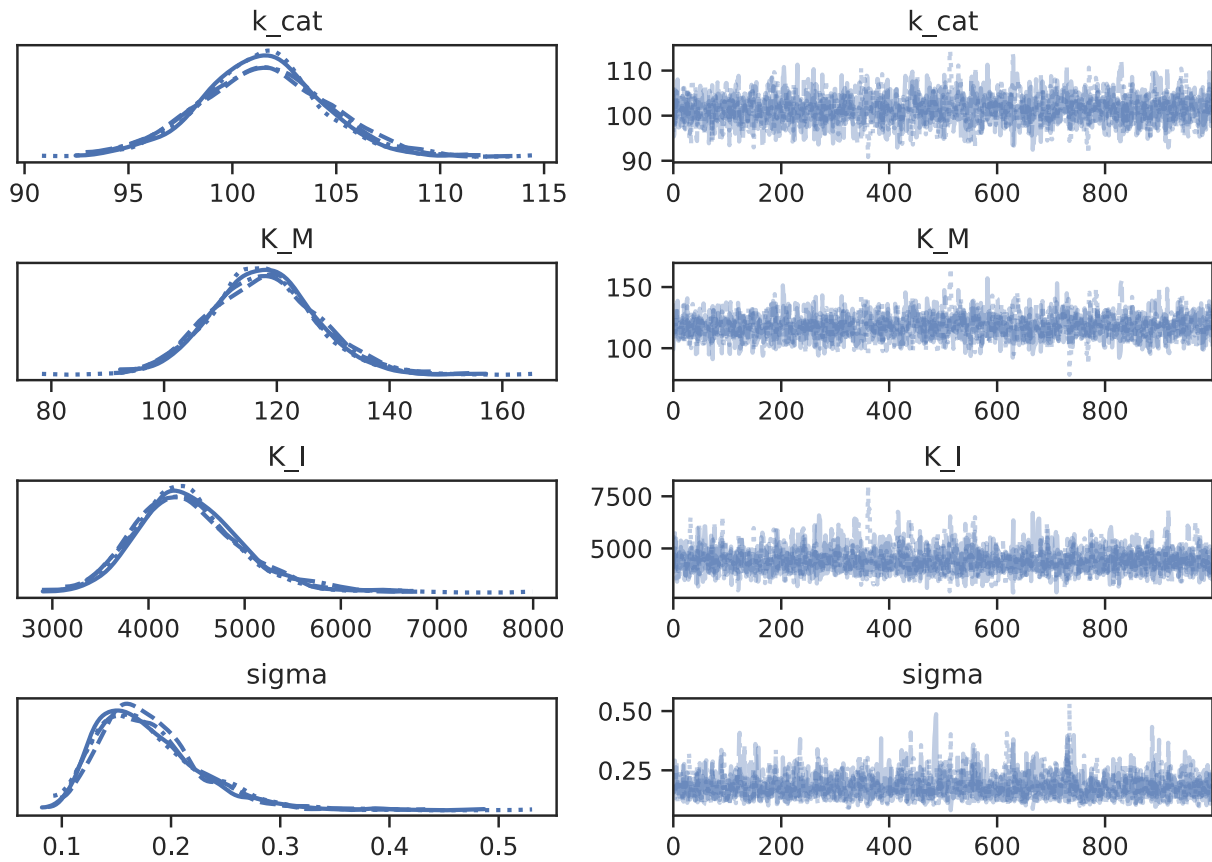


Figure S5: Diagnostic sampling trace plots of all kinetic parameters inferred in manuscript Figure 1

## Combining diverse experimental datasets

### Model

The system of GDH and HK PEBs was modeled as a competitive two-reaction system, where GDH catalyses the reaction  $G + NAD \rightarrow GdL + NADH$ , and HK catalyses  $G + ATP \rightarrow G6P + ADP$ . This system is described by the following set of ODE's:

$$\mathbf{f}(\mathbf{C}, \phi, \theta) : \begin{cases} \frac{d[G]}{dt} = -\frac{[GDH] \cdot k_{cat}^{GDH} \cdot [G][NAD]}{1+[G]/K_G^{GDH}+[NAD]/K_{NAD}^{GDH}} - \frac{[HK] \cdot k_{cat}^{HK} \cdot [G][ATP]}{1+[G]/K_G^{HK}+[ATP]/K_{ATP}^{HK}} - k_f([G] - [G]_{in}) \\ \frac{d[GdL]}{dt} = \frac{[GDH] \cdot k_{cat}^{GDH} \cdot [G][NAD]}{1+[G]/K_G^{GDH}+[NAD]/K_{NAD}^{GDH}} - k_f[P] - k_f[GdL] \\ \frac{d[G6P]}{dt} = \frac{[HK] \cdot k_{cat}^{HK} \cdot [G][ATP]}{1+[G]/K_G^{HK}+[ATP]/K_{ATP}^{HK}} - k_f[G6P] \\ \frac{d[NAD]}{dt} = -\frac{[GDH] \cdot k_{cat}^{GDH} \cdot [G][NAD]}{1+[G]/K_G^{GDH}+[NAD]/K_{NAD}^{GDH}} - k_f([NAD] - [NAD]_{in}) \\ \frac{d[NADH]}{dt} = \frac{[GDH] \cdot k_{cat}^{GDH} \cdot [G][NAD]}{1+[G]/K_G^{GDH}+[NAD]/K_{NAD}^{GDH}} - k_f[NADH] \\ \frac{d[ATP]}{dt} = -\frac{[HK] \cdot k_{cat}^{HK} \cdot [G][ATP]}{1+[G]/K_G^{HK}+[ATP]/K_{ATP}^{HK}} - k_f([ATP] - [ATP]_{in}) \\ \frac{d[ADP]}{dt} = \frac{[HK] \cdot k_{cat}^{HK} \cdot [G][ATP]}{1+[G]/K_G^{HK}+[ATP]/K_{ATP}^{HK}} - k_f[ADP] \end{cases}$$

Depending on the experiment, either the  $[NADH]$  concentration or the  $[ATP]$  concentration at steady-state are observed, from which the 6 kinetic parameters are inferred,  $\phi = \{k_{cat}^{GDH}, K_G^{GDH}, K_{NAD}^{GDH}, k_{cat}^{HK}, K_G^{HK}, K_{ATP}^{HK}\}$ . In every experiment, 6 control parameters exist:  $\theta = \{[GDH], [HK], k_f, [G]_{in}, [NAD]_{in}, [ATP]_{in}, \}$ . The measurements of the observed product concentration are assumed to have normal-distributed noise  $[P]_{obs} \sim N([P]_{ss}, \sigma)$  with a mean equal to the true steady-state concentration and an unknown standard-deviation  $\sigma$ . As priors for the 4 Michaelis kinetic parameters, uninformative uniform distributions are used, with the following upper and lower boundaries:

$$\begin{aligned} P(K_G^{GDH}) &= \mathcal{U}(1, 20000) \\ P(K_{NAD}^{GDH}) &= \mathcal{U}(1, 20000) \\ P(K_G^{HK}) &= \mathcal{U}(1, 4000) \\ P(K_{ATP}^{HK}) &= \mathcal{U}(1, 6000) \end{aligned}$$

The 0-value was not included in the domain of these priors because it is highly unlikely and causes problems with divergent sampling.

The turn-over number  $k_{cat}$  is not only different for both enzymes, but can also vary between batch of enzymes or PEB's. To somewhat constrain the inferred values and ensure that the sampler can properly converge, the priors were modelled as uniform distributions with an upper boundary sampled from a gamma-distribution.

As priors for the noise estimate sigmas for each experiment, an exponential distribution was used. To help the sampling procedure, an exponential hyperprior was used for the distribution parameters.

### Diagnostics

Chains	Tuning steps	Draws	Mean acceptance rate	Divergences
0	8	1000	0.974	5

	mcse_mean	mcse_sd	ess_bulk	ess_tail	r_hat
k_cat_hyper	10.3	7.29	1163.0	1714.0	1.0
k_GDH_cat[1]	0.07	0.05	4374.0	3463.0	1.0
k_GDH_cat[2]	0.31	0.23	4159.0	3295.0	1.0

	mcse_mean	mcse_sd	ess_bulk	ess_tail	r_hat
k_GDH_cat[3]	0.06	0.04	4464.0	3944.0	1.0
k_HK_cat	0.47	0.39	4972.0	2798.0	1.0
K_GDH_G	20.52	15.48	4518.0	3262.0	1.0
K_GDH_NAD	0.75	0.62	4937.0	4050.0	1.0
K_HK_G	3.5	2.47	2120.0	3584.0	1.0
K_HK_ATP	13.33	11.48	2030.0	2290.0	1.0
sigma	0.0	0.0	7195.0	5833.0	1.0
sigma_HK[SNCA17]	1.39	0.98	2462.0	3719.0	1.0
sigma_HK[SNCA18]	1.44	1.08	7794.0	5116.0	1.0
sigma_HK[SNKS03]	0.58	0.41	2484.0	4945.0	1.0
sigma_HK[SNKS04]	0.77	0.55	2726.0	4230.0	1.0
sigma_GDH[SNCA14]	0.48	0.39	6051.0	3925.0	1.0
sigma_GDH[SNCA15]	0.3	0.22	6236.0	4164.0	1.0
sigma_GDH[SNKS11]	0.48	0.38	8520.0	4796.0	1.0
sigma_GDH[SNKS12]	0.5	0.39	8737.0	5330.0	1.0
sigma_GDH[SNKS18]	0.11	0.08	5624.0	4523.0	1.0
sigma_HK_GDH_1[SNKS06]	1.22	0.91	8526.0	5309.0	1.0
sigma_HK_GDH_2[SNNS002]	0.02	0.01	4710.0	4867.0	1.0
sigma_HK_GDH_2[SNNS003]	0.19	0.14	7393.0	3944.0	1.0
sigma_HK_GDH_2[SNNS004]	0.06	0.05	6504.0	4159.0	1.0
sigma_HK_GDH_2[SNNS005]	0.2	0.15	7370.0	4777.0	1.0
sigma_HK_GDH_2[SNNS006]	0.44	0.34	8358.0	3739.0	1.0
sigma_HK_GDH_2[SNNS007]	0.16	0.12	8927.0	5406.0	1.0

## Comparing reaction mechanism hypotheses

### Models

The system of G6PDH PEB's was modeled as the reaction  $\text{G6p} + \text{NAD} \rightarrow \text{G6PdL} + \text{NADH}$ . Every hypothesis under investigation followed a different proposed rat equation, but the priors were kept as equivalent uninformative priors for every hypothesis:

$$\begin{aligned} P(k_{cat}) &= \mathcal{U}(0, 500) \\ P(K_{NAD}) &= \mathcal{U}(1, 4000) \\ P(K_{G6P}) &= \mathcal{U}(1, 2000) \\ P(K_{I,NADH}) &= \mathcal{U}(1, 10000) \end{aligned}$$

As prior for the noise estimate sigma, an uninformative exponential distribution was used:

$$P(\sigma) = \text{Exp}(0.5)$$

### Hypothesis 0

Table S8: Sampling statistics for manuscript Figure 5, Hypothesis 0

Chains	Tuning steps	Draws	Mean acceptance rate	Divergences
0	4	1000	1000	0.959

Table S9: Sampling diagnostics for manuscript Figure 5, Hypothesis 0

	mcse_mean	mcse_sd	ess_bulk	ess_tail	r_hat
k_cat	0.04	0.03	1630	1921	1
K_G6P	1.54	1.09	2013	2446	1
K_NAD	0.73	0.52	2082	2219	1
sigma[SNKS08]	0.12	0.08	2733	2260	1
sigma[SNKS20]	0.11	0.08	3153	2671	1

### Hypothesis 1

Table S10: Sampling statistics for manuscript Figure 5, Hypothesis 1

Chains	Tuning steps	Draws	Mean acceptance rate	Divergences
0	4	1000	1000	0.94

Table S11: Sampling diagnostics for manuscript Figure 5, Hypothesis 1

	mcse_mean	mcse_sd	ess_bulk	ess_tail	r_hat
k_cat	3.1	2.2	122	417	1.02
K_G6P	62.29	44.16	127	482	1.02
K_NAD	11.85	8.91	317	413	1.02
KI_NADH	259.12	183.58	189	435	1.02
sigma[SNKS08]	1.68	1.19	127	491	1.03
sigma[SNKS20]	1.75	1.24	123	277	1.02

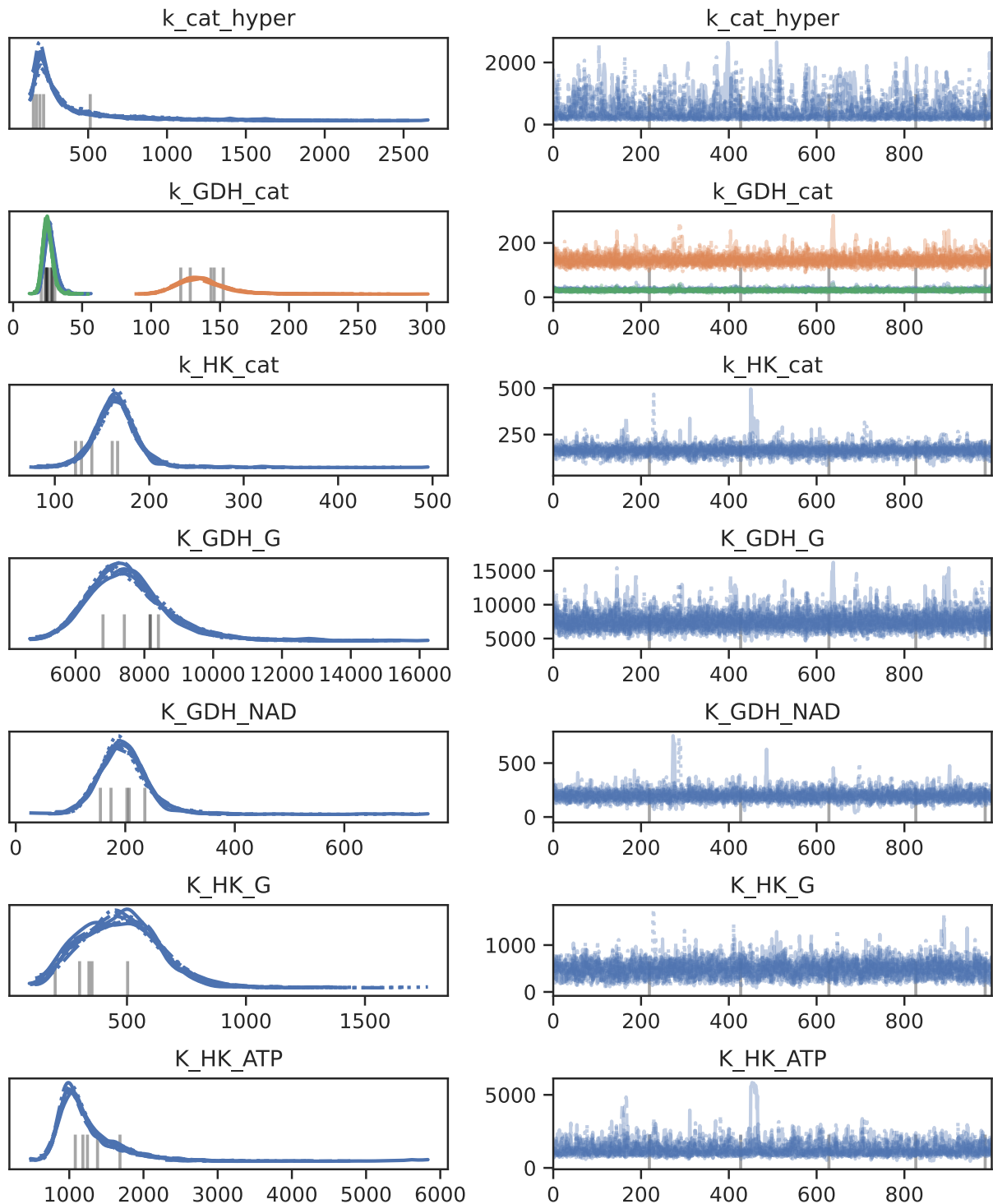


Figure S6: Diagnostic sampling trace plots of all kinetic parameters inferred in manuscript Figure 3

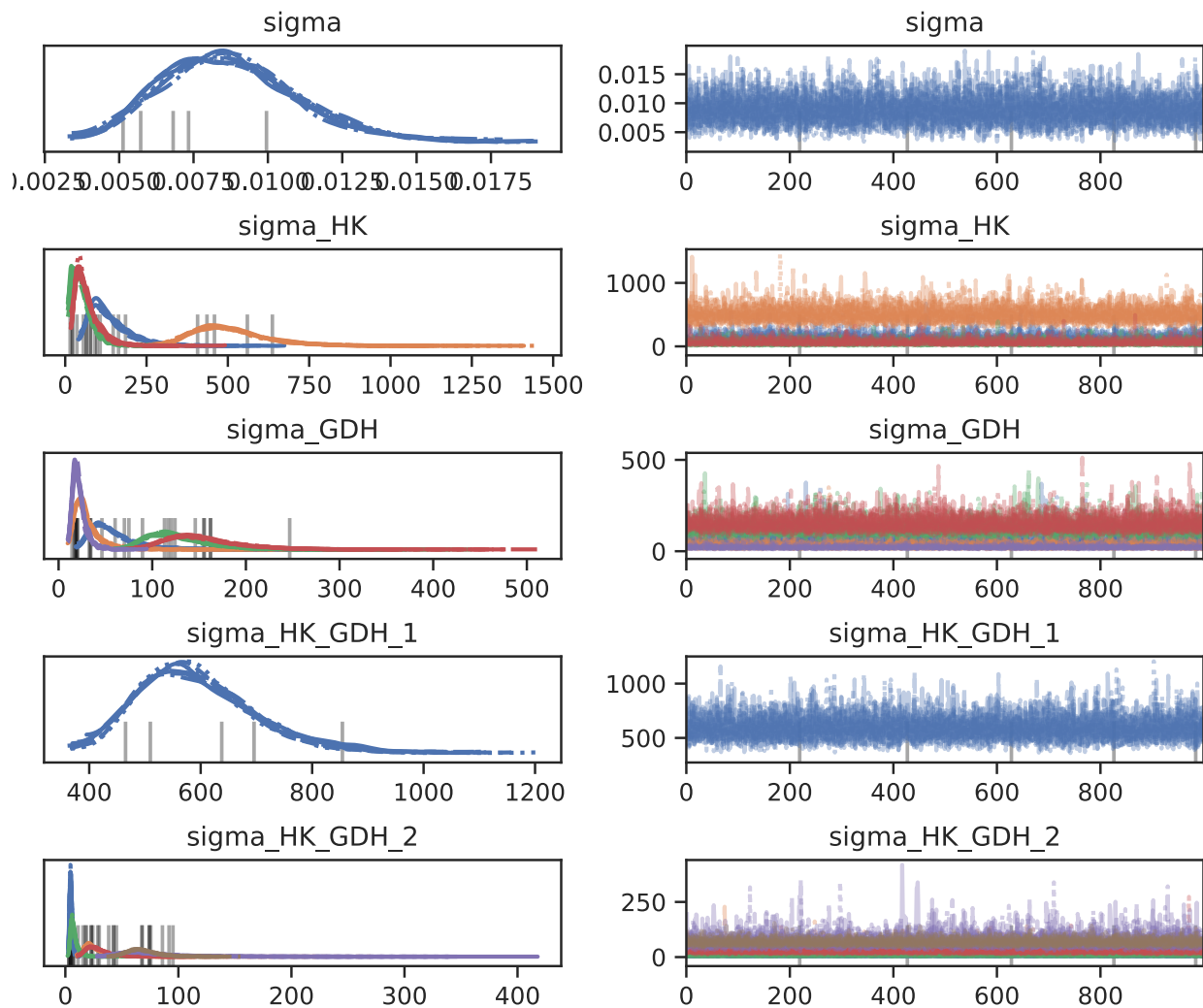


Figure S7: Diagnostic sampling trace plots of all uncertainty estimates inferred in manuscript Figure 3

## Hypothesis 2

Table S12: Sampling statistics for manuscript Figure 5, Hypothesis 2

Chains	Tuning steps	Draws	Mean acceptance rate	Divergences
0	4	1000	1000	0.946

Table S13: Sampling diagnostics for manuscript Figure 5, Hypothesis 2

	mcse_mean	mcse_sd	ess_bulk	ess_tail	r_hat
k_cat	0.47	0.34	729	578	1
K_G6P	8.34	6.08	843	928	1
K_NAD	3.14	2.24	935	828	1
KI_NADH	9.97	8.11	1119	749	1
sigma[SNKS08]	0.24	0.17	1189	1405	1
sigma[SNKS20]	0.23	0.17	808	1000	1

## Hypothesis 3

Table S14: Sampling statistics for manuscript Figure 5, Hypothesis 3

Chains	Tuning steps	Draws	Mean acceptance rate	Divergences
0	4	1000	1000	0.945

Table S15: Sampling diagnostics for manuscript Figure 5, Hypothesis 3

	mcse_mean	mcse_sd	ess_bulk	ess_tail	r_hat
k_cat	0.45	0.34	1034	981	1.01
K_G6P	7.24	5.45	1195	1214	1
K_NAD	2.66	2.11	1421	1275	1
KI_NADH	5.36	3.86	1894	2034	1
sigma[SNKS08]	0.21	0.15	1441	1201	1
sigma[SNKS20]	0.15	0.1	1216	1226	1

## Hypothesis 4

Table S16: Sampling statistics for manuscript Figure 5, Hypothesis 4

Chains	Tuning steps	Draws	Mean acceptance rate	Divergences
0	4	1000	1000	0.948

Table S17: Sampling diagnostics for manuscript Figure 5, Hypothesis 4

	mcse_mean	mcse_sd	ess_bulk	ess_tail	r_hat
k_cat	0.35	0.25	1199	1621	1
K_G6P	5.93	4.29	1371	1644	1

	mcse_mean	mcse_sd	ess_bulk	ess_tail	r_hat
K_NAD	1.69	1.21	1881	2357	1
KI_NADH	9.91	7.15	1901	2094	1
sigma[SNKS08]	0.15	0.1	2068	2340	1
sigma[SNKS20]	0.1	0.07	2175	2106	1

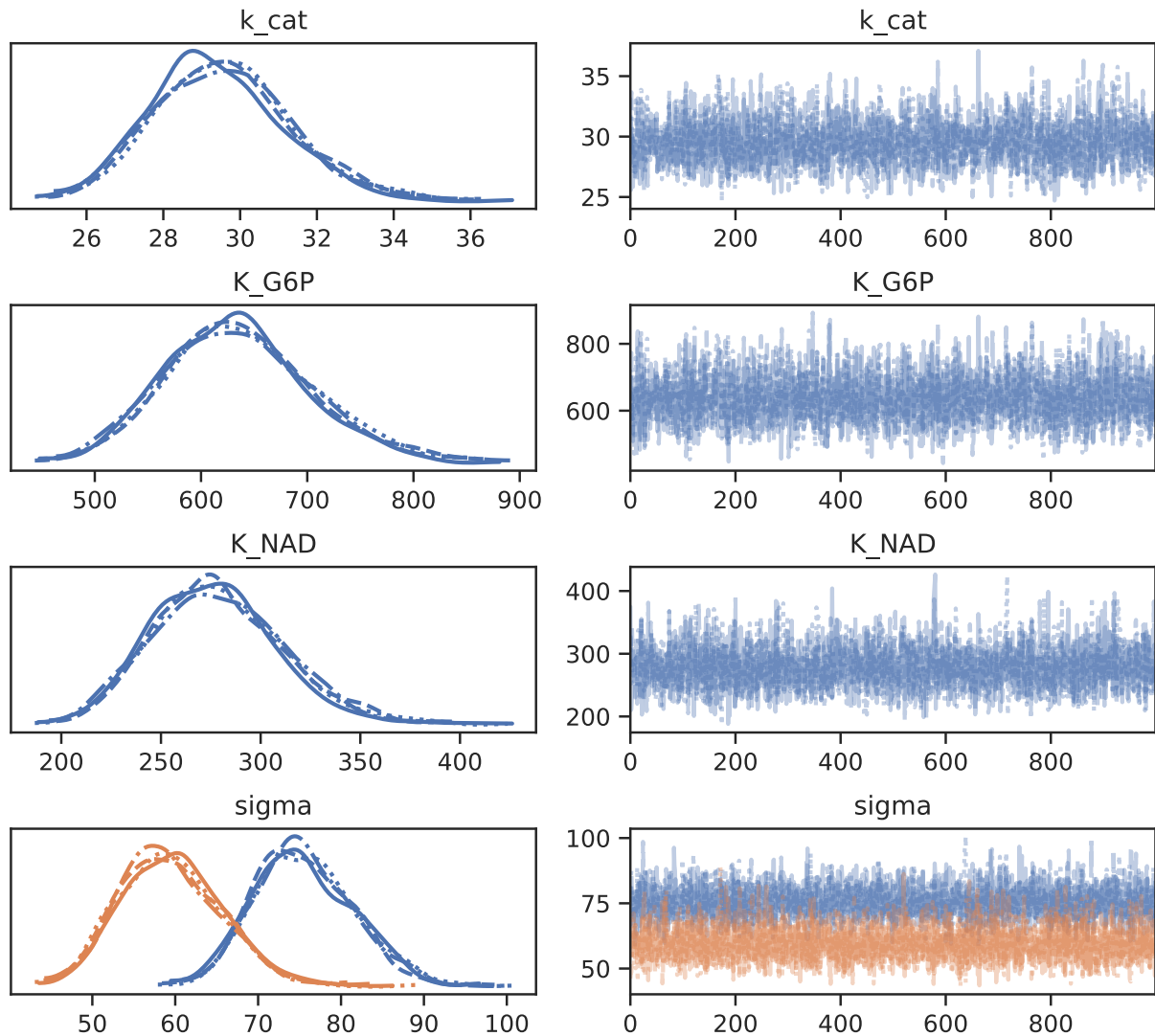


Figure S8: Diagnostic sampling trace plots of kinetic parameters inferred in manuscript Fig. 5, Hypothesis 0

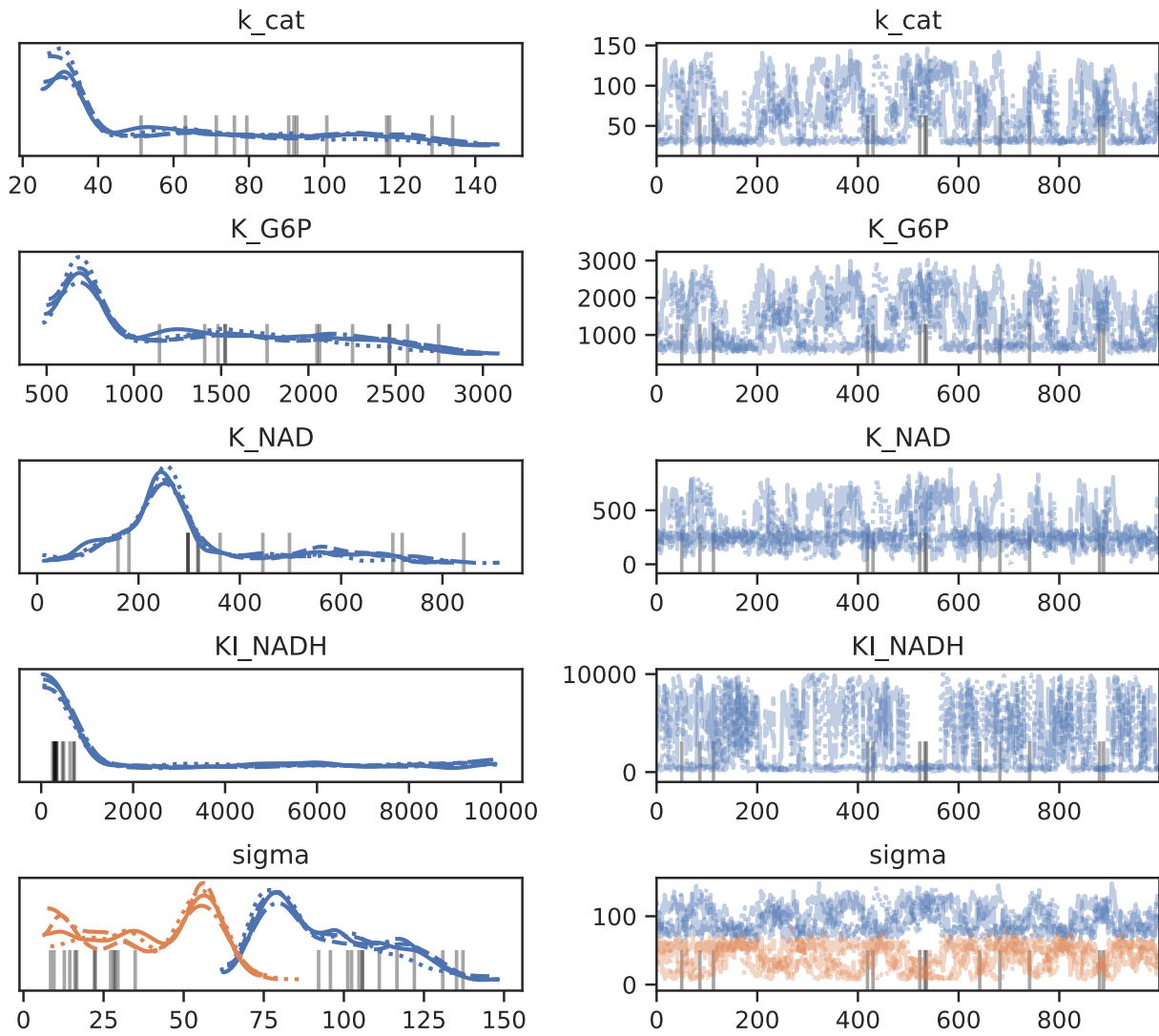


Figure S9: Diagnostic sampling trace plots of kinetic parameters inferred in manuscript Fig. 5, Hypothesis 1

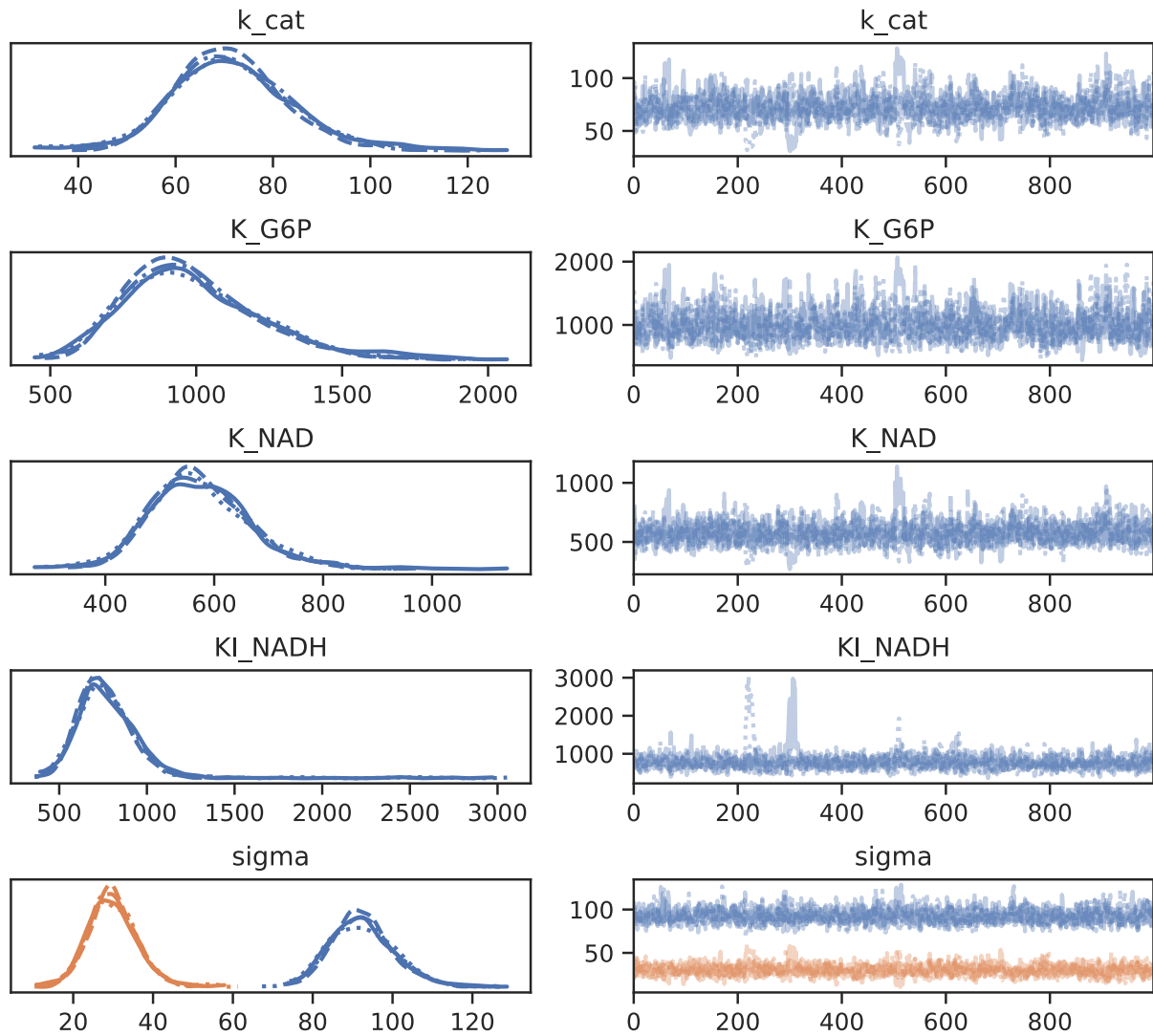


Figure S10: Diagnostic sampling trace plots of kinetic parameters inferred in manuscript Fig. 5, Hypothesis 2

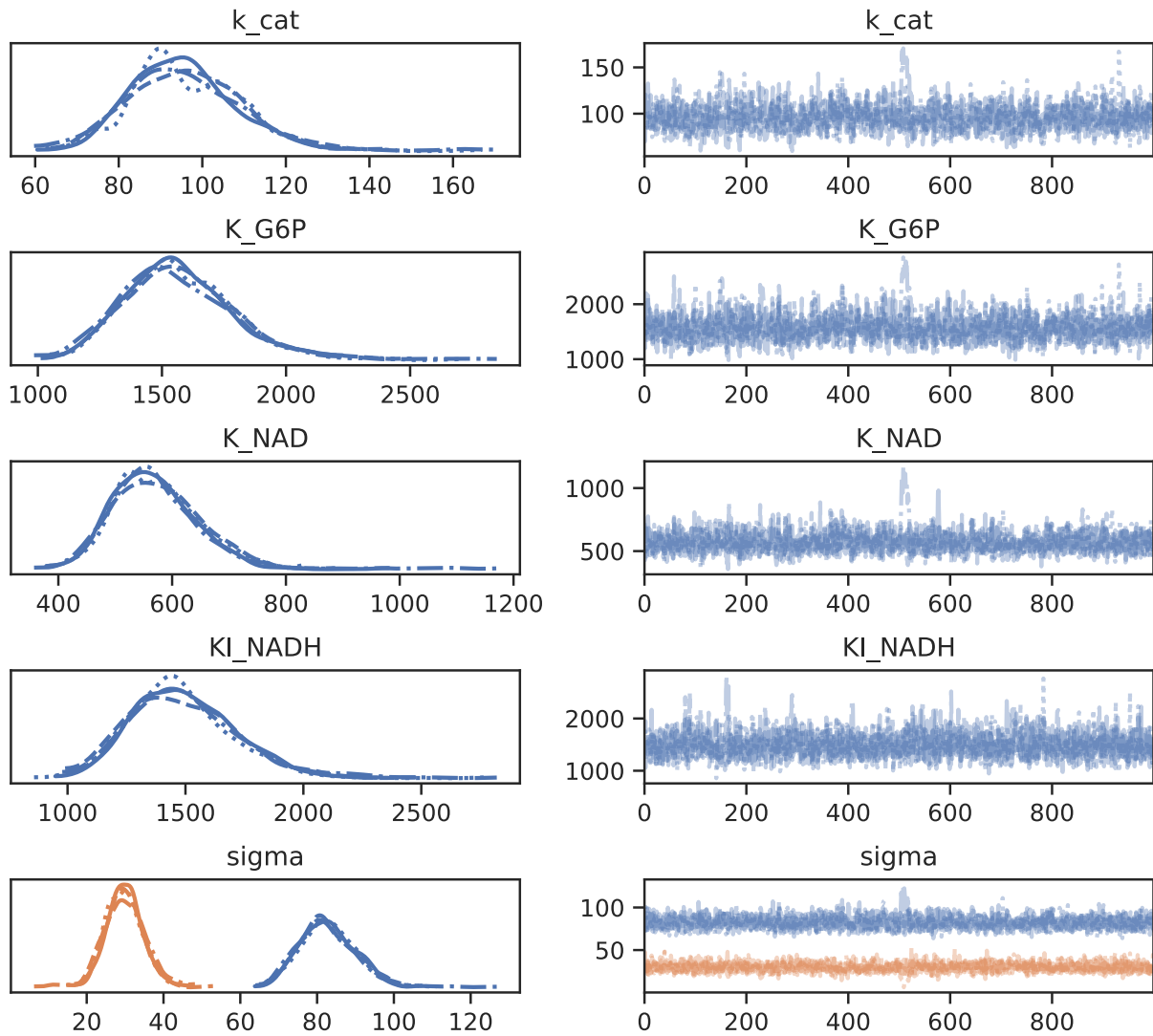


Figure S11: Diagnostic sampling trace plots of kinetic parameters inferred in manuscript Fig. 5, Hypothesis 3

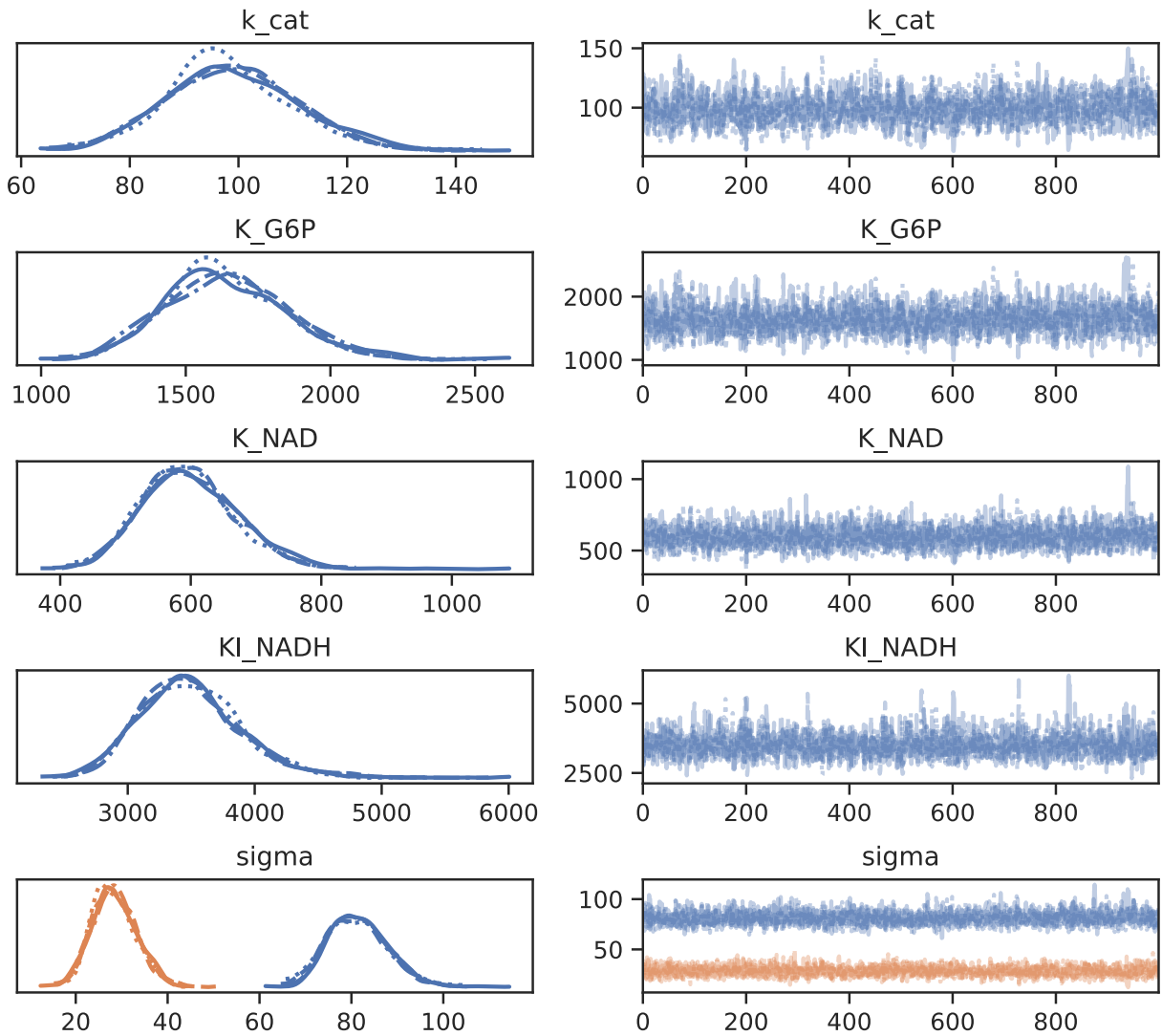


Figure S12: Diagnostic sampling trace plots of kinetic parameters inferred in manuscript Fig. 5, Hypothesis 4

->

## References

- (1) Klein, A. M.; Mazutis, L.; Akartuna, I.; Tallapragada, N.; Veres, A.; Li, V.; Peshkin, L.; Weitz, D. A.; Kirschner, M. W. Droplet Barcoding for Single-Cell Transcriptomics Applied to Embryonic Stem Cells. *Cell* **2015**, *161* (5), 1187–1201. <https://doi.org/10.1016/j.cell.2015.04.044>.
- (2) Matula, K.; Rivello, F.; Huck, W. T. S. Single-Cell Analysis Using Droplet Microfluidics. *Advanced Biosystems* **2020**, *4* (1), 1900188. <https://doi.org/10.1002/adbi.201900188>.
- (3) Semenov, S. N.; Markvoort, A. J.; Gevers, W. B. L.; Piruska, A.; Greef, T. F. A. de; Huck, W. T. S. Ultrasensitivity by Molecular Titration in Spatially Propagating Enzymatic Reactions. *Biophysical Journal* **2013**, *105* (4), 1057–1066. <https://doi.org/10.1016/j.bpj.2013.07.002>.
- (4) Salvatier, J.; Wiecki, T. V.; Fonnesbeck, C. Probabilistic Programming in Python Using PyMC3. *PeerJ Computer Science* **2016**, *2*, e55. <https://doi.org/10.7717/peerj-cs.55>.
- (5) Hoffman, M. D.; Gelman, A. The No-U-Turn Sampler: Adaptively Setting Path Lengths in Hamiltonian Monte Carlo. *arXiv:1111.4246 [cs, stat]* **2011**.
- (6) Virtanen, P.; Gommers, R.; Oliphant, T. E.; Haberland, M.; Reddy, T.; Cournapeau, D.; Burovski, E.; Peterson, P.; Weckesser, W.; Bright, J.; Walt, S. J. van der; Brett, M.; Wilson, J.; Millman, K. J.; Mayorov, N.; Nelson, A. R. J.; Jones, E.; Kern, R.; Larson, E.; Carey, C. J.; Polat, İ.; Feng, Y.; Moore, E. W.; VanderPlas, J.; Laxalde, D.; Perktold, J.; Cimrman, R.; Henriksen, I.; Quintero, E. A.; Harris, C. R.; Archibald, A. M.; Ribeiro, A. H.; Pedregosa, F.; Mulbregt, P. van; Vijaykumar, A.; Bardelli, A. P.; Rothberg, A.; Hilboll, A.; Kloeckner, A.; Scopatz, A.; Lee, A.; Rokem, A.; Woods, C. N.; Fulton, C.; Masson, C.; Häggström, C.; Fitzgerald, C.; Nicholson, D. A.; Hagen, D. R.; Pasechnik, D. V.; Olivetti, E.; Martin, E.; Wieser, E.; Silva, F.; Lenders, F.; Wilhelm, F.; Young, G.; Price, G. A.; Ingold, G.-L.; Allen, G. E.; Lee, G. R.; Audren, H.; Probst, I.; Dietrich, J. P.; Silterra, J.; Webber, J. T.; Slavić, J.; Nothman, J.; Buchner, J.; Kulick, J.; Schönberger, J. L.; Miranda Cardoso, J. V. de; Reimer, J.; Harrington, J.; Rodríguez, J. L. C.; Nunez-Iglesias, J.; Kuczynski, J.; Tritz, K.; Thoma, M.; Newville, M.; Kümmeler, M.; Bolingbroke, M.; Tartre, M.; Pak, M.; Smith, N. J.; Nowaczyk, N.; Shebanov, N.; Pavlyk, O.; Brodtkorb, P. A.; Lee, P.; McGibbon, R. T.; Feldbauer, R.; Lewis, S.; Tygier, S.; Sievert, S.; Vigna, S.; Peterson, S.; More, S.; Pudlik, T.; Oshima, T.; Pingel, T. J.; Robitaille, T. P.; Spura, T.; Jones, T. R.; Cera, T.; Leslie, T.; Zito, T.; Krauss, T.; Upadhyay, U.; Halchenko, Y. O.; Vázquez-Baeza, Y. SciPy 1.0: Fundamental Algorithms for Scientific Computing in Python. *2020*, *17* (3), 261–272. <https://doi.org/10.1038/s41592-019-0686-2>.